Analysis, Design, and Prototype Testing of a Smooth-Walled Box Culvert System

RAYMOND B. SEED, JONATHAN D. BRAY, AND DAVID C. THOMAS

The smooth-walled box structure system described in this paper represents a new approach to the problem of providing efficient transport of water beneath ground cover with limited crown clearances. The smooth walls of these structures provide significantly increased hydraulic efficiency over that achieved by current conventional corrugated metal box culverts. This hydraulic efficiency offsets the decreased structural efficiency (decreased flexural capacity) of the composite smooth plate/rib section and permits the use of a significantly smaller smooth-walled box structure cross-sectional area to transport the same maximum design flow volume as would be transported by a significantly larger corrugated box culvert cross-sectional area. Use of this smooth-walled box structure, in turn, minimizes overall structure size and cost, requires smaller clearances for installation under shallow cover constraints, and minimizes the excavation and backfill volumes required for installation. A summary of the studies involved in the analysis and preliminary design and testing of this new type of box culvert system is presented in this paper. Included are an overview of the design procedures used to develop the new smooth-walled box structural system, a summary of the scale-model hydraulic testing program performed to evaluate hydraulic performance, a summary of the results of full-scale laboratory structural tests of the various new box culvert system components, and a discussion of finite element analyses performed to evaluate the proposed new culvert system. In addition, a full-scale prototype structure was constructed, backfilled, and then subjected to repeated cycles of HS-20 design loading. The results of this full-scale prototype test, as well as finite element analyses of this test, are also presented and discussed.

The SmoothWall™ Box Structure is a recently proposed type of flexible aluminum box culvert system designed to provide hydraulically efficient transport of fluids under relatively shallow surface cover. The new system is unique inasmuch as the proposed new smooth-walled box structures develop the flexural stiffness and bending moment capacities required to withstand backfill and live surface loads by means of external ribs bolted to the smooth plates that form the box structure perimeters. This system is in contrast to the heretofore conventional approach of using corrugated structural plate (with or without ribs) to provide some or all of the flexural strength and stiffness required for conventional corrugated box culverts.

The principal advantage of the new smooth-walled box structure system is the decreased hydraulic roughness of the smooth walls as compared with conventional corrugated plate wall systems. This decrease in hydraulic roughness improves the hydraulic efficiency of the system and permits the use of a significantly smaller smooth-walled box structure cross-sectional area to transport the same maximum design flow volume as would be transported by a significantly larger corrugated box culvert cross-sectional area. This smaller structure, in turn, minimizes the excavation and backfill volumes required for installation, requires smaller clearances for installation near obstructions and under shallow cover constraints, reduces overall structure size and cost, and offsets the reduced flexural structural efficiency associated with the use of smooth rather than corrugated structural plate.

R. B. Seed and J. D. Bray, Department of Civil Engineering, University of California, Berkeley, Calif. 94720. D. C. Thomas, Gator Culvert, 865 N. Dixie Highway, Lantana, Fla. 33465.

NEW SMOOTH-WALLED BOX STRUCTURES

A typical cross section through a SmoothWall™ Box Structure is shown in Figure 1a. The proposed new smooth-walled box structures will initially have cross-sectional shapes similar to those currently used for conventional corrugated metal box culverts. Initial spans range from approximately 9 ft, 3 in. to 16 ft, 3 in., with rises ranging from 2 ft, 2 in. to 6 ft, 2 in. The perimeters or shells of the new structures consist of smooth, noncorrugated aluminum structural plate 0.125 in. thick. Flexural stiffness and strength are provided by bolting external stiffening ribs to the smooth plate at regular intervals. These stiffening ribs necessarily extend around the full perimeter of the culvert and occur at longitudinal spacings of 6-, 8-, 12-, or 16-in. on center (o.c.) depending on required flexural capacities.

The hydraulic roughness of this system is controlled principally by cross section geometry and scale and by the locations, spacing, and configuration of the bolt heads, which must protrude into the culvert interior in order to (a) connect plates at plate joints or laps, and (b) affix the external bracing ribs. To further improve the hydraulic efficiency of the smooth-walled hydraulic box structures, a new streamlined bolt head is employed on the interior of the new structures. A profile view of the hexagonal head of the ¾-in.-diameter steel bolts used in assembling conventional corrugated aluminum culverts and the streamlined internally protruding bolt head used in assembling the smooth-walled box structures are shown in Figure 2. The total protruding bolt head height is reduced, and the streamlined bolt heads are provided with rounded tops. These modifications have no detrimental impact on bolt performance as a high-strength fastener.

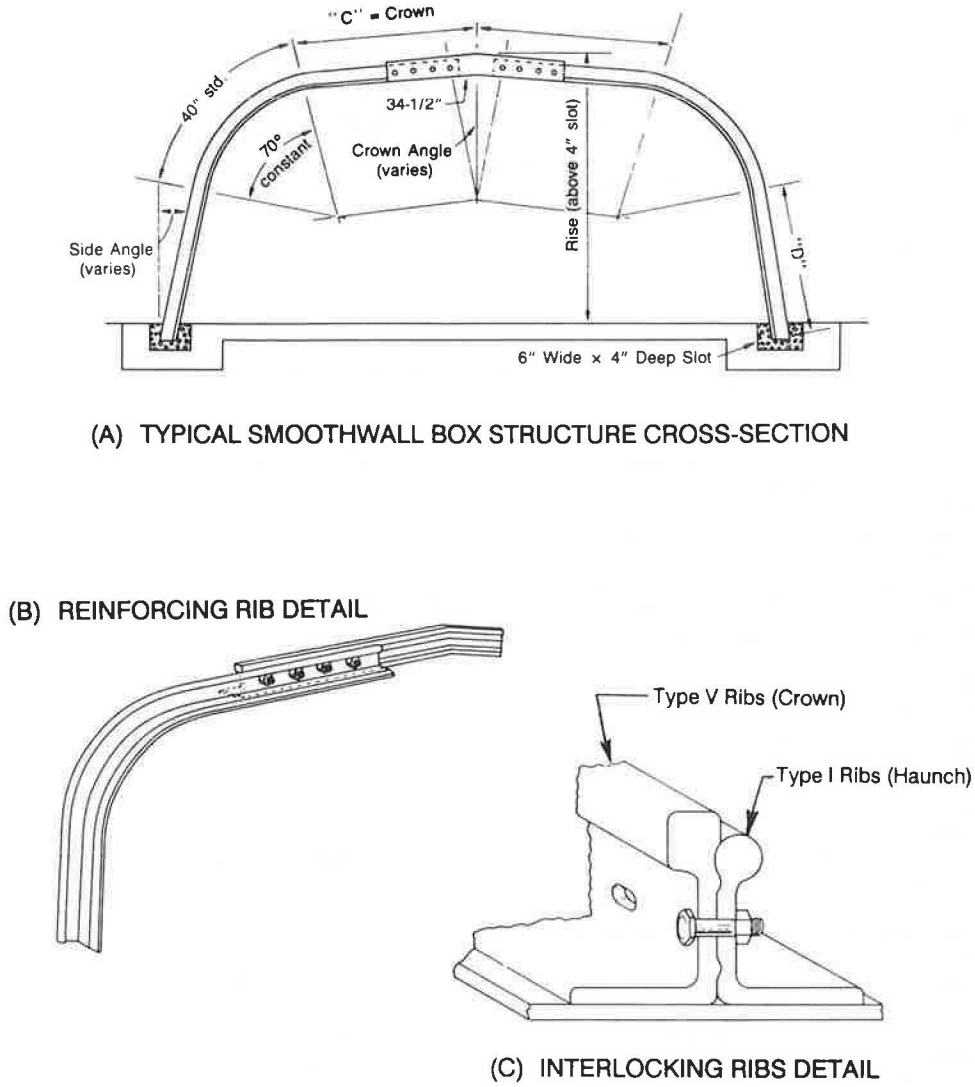

FIGURE 1 Schematic illustration of a typical smooth-walled box structure (after Kaiser Drainage Products).

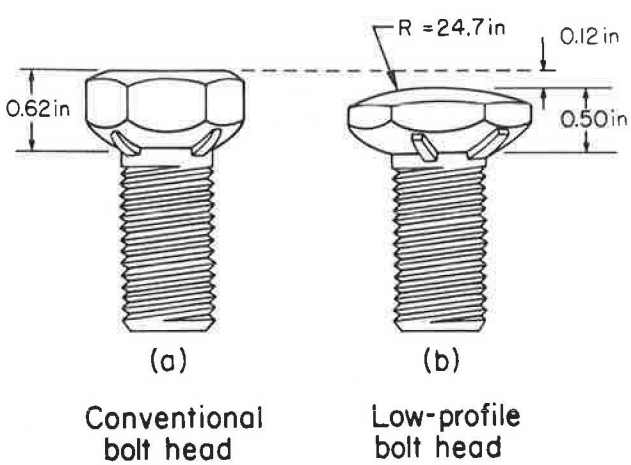

FIGURE 2 Profile view of conventional and streamlined bolt heads.

HYDRAULIC SCALE MODEL TESTS

Scale model hydraulic tests were performed in the large-scale hydraulic flume at San Jose State University to evaluate the hydraulic efficiency of the new smooth-walled box structures (*1*). This hydraulic flume is 47.5 in. wide, 36 in. deep, and approximately 38 ft long. A scaling factor of 1:5 was selected for the scale model hydraulic testing because this factor permitted representative testing of scale models of selected conventional corrugated box culverts and smooth-walled box structure sections.

A total of four box culvert cross sections were subjected to one-fifth-scale model hydraulic tests. Two of these were scale models of conventional corrugated box culverts, and two were scale models of smooth-walled box structures. The two conventional corrugated box culvert sections were tested to provide a basis for evaluating possible scaling effects as well as the overall reliability of the scale model testing procedures

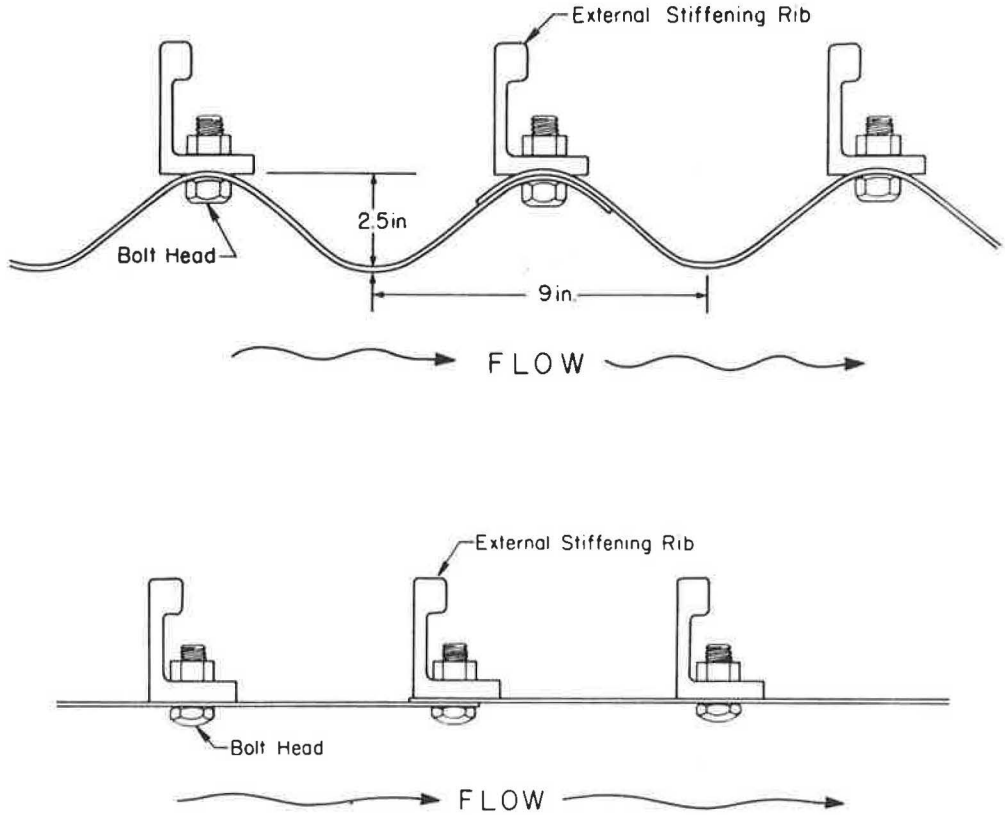

FIGURE 3 Schematic illustration of corrugated box culvert and smooth-walled box structure wall configurations.

employed. A schematic illustration of the walls of (a) conventional corrugated aluminum box culverts and (b) the new smooth-walled box structures is presented in Figure 3. In this illustration, the differences in hydraulic roughness between the two culvert systems can be clearly seen.

A schematic illustration of a typical scale model box culvert hydraulic test configuration is presented in Figure 4. All tests were performed under steady-state flow conditions with the sections flowing full. Flow velocities were selected so that, after allowance for appropriate scaling effects, flow characteristics in the hydraulic models would be representative of anticipated field conditions at maximum design flow. Each cross section was tested with three different total lengths, but with identical flow rates, so that energy losses associated with entrance and exit conditions could be separated from energy losses associated with internal roughness conditions. The interiors of both the corrugated and smooth-walled box culverts were accurately modeled to one-fifth scale, including all significant details such as corrugations, plate laps, and internally protruding bolt heads.

By using the results of these scale model tests, the new smooth-walled box structures were found to have Manning's n-values of less than $n = 0.015$, and a value of $n = 0.015$ was conservatively selected for hydraulic design. This finding represents a considerable improvement in hydraulic efficiency over the values of $n \approx 0.032$ to 0.035 used for hydraulic design of existing conventional corrugated aluminum box culverts.

LABORATORY STRUCTURAL TESTING

Following completion of conceptual design and preliminary development of system component configurations, the next step in the design process involved identification of potential system failure modes. Three such modes were identified: (a) potential compressive failure of the lower haunch region (in thrust), (b) potential flexural (bending moment) failure of the crown or haunch regions, and (c) potential bolt pull-through or excessive deformations of the smooth structural lining plate under normal (radial) exterior pressures. The first two failure modes are common to the design of conventional corrugated metal box culverts, but the third potential failure mode is unique to the new smooth-walled box structures.

Large-scale structural tests of culvert system components were performed to evaluate the capacities of the various components to resist these potential failure modes. The resulting design capacities were then used, along with design procedures based on finite element method (FEM) analyses, to finalize the design of a family of smooth-walled box structures of varying spans and rises.

The large-scale laboratory tests were performed at the Kaiser Center for Technology on assembled full-scale prototype culvert sections to evaluate the following structural design capacities: flexural capacities, bolt pull-through capacity, and plate deformations under applied exterior normal pressures. No tests were performed to evaluate haunch section thrust

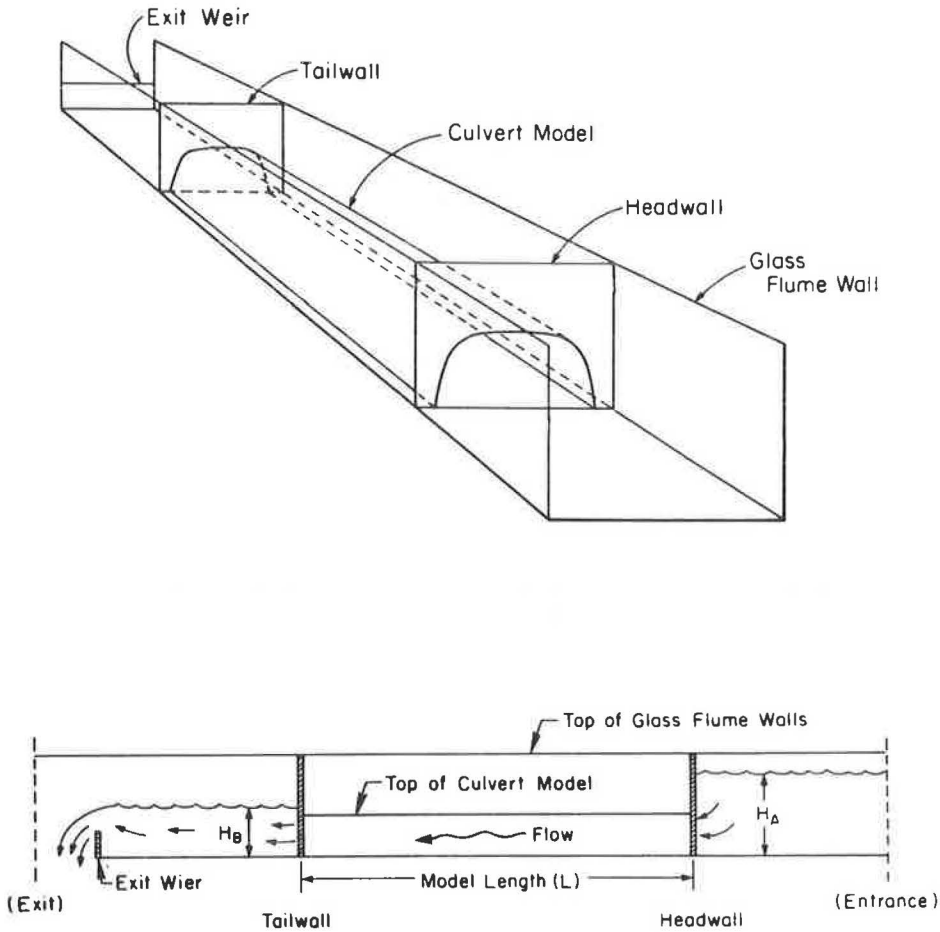

FIGURE 4 Schematic illustration of typical scale model box culvert hydraulic test configuration.

capacities because the axial load capacities of the haunch ribs had been established in previous studies, and the axial rib capacities alone proved to be more than adequate to safely sustain the largest anticipated haunch thrust loads.

The new smooth-walled box culverts employ a Type V aluminum bulb angle rib across the central crown section, and a light Type I rib along the haunches and ends of the crown section, as illustrated in Figures 1b and 1c. These two ribs are designed to "mate" and provide a positive moment connection at the juncture (splice) locations, as shown in Figure 1c. Ribs occur at spacings of 6-, 8-, 12-, or 16-in. o.c., depending on required flexural capacities.

Flexural tests were performed on assembled crown and haunch sections and on assembled Type I/Type V rib splice sections. All tests were performed on sections of 0.125-in. aluminum plate with reinforcing ribs bolted on at spacings of 8- or 16-in. o.c., and all composite plate/rib sections were tested in 32-in. widths to mobilize fully representative bolt shear at the plate/rib contacts. All composite plate/rib sections were tested as simply supported spans of 60 in. with a pair of centrally applied parallel line loads spaced at 11-in.

The results of these flexural tests and a comparison of the measured flexural capacities (M_{ult}) and the calculated theoretical capacities (M_p) are presented in Table 1. Calculation of the theoretical M_p for each composite plate/rib section was based on assumption of full composite plate/rib section behavior, and assumed nominal yield stresses of σ_y = 24 ksi for the plate and σ_y = 35 ksi for the ribs. As shown in Table 1 (a–c), the measured capacities for composite plate/rib sections with both Type I and Type V ribs were higher than the theoretical capacities. Accordingly, the theoretical plastic moment capacities (M_p) were conservatively adopted as a basis for design. The measured flexural capacities of the Type I/Type V splice zones were found to be intermediate between that of Type I plate/rib sections and Type V plate/rib sections (Table 1). Accordingly, the splice sections were conservatively assigned the same design capacities as Type I composite plate/rib sections. The resulting design moment capacities, based on these flexural tests, are presented in Table 2. It should be noted that these design moment capacities are based on assumed nominal yield stresses of σ_y = 24 ksi for the plate and σ_y = 35 ksi for the ribs.

A second set of laboratory tests was performed to evaluate the resistance of the 0.125-in. aluminum structural plate to failure by bolt pull-through, defined as punching failure of the bolt head when pulled through the plate. Square plate sections 16-in. by 16-in. were fixed at their four corners, and a single bolt was installed in the center of the plate. This bolt was then pulled out through the plate. Two series of bolt pull-through tests were performed, one with the bolt nuts torqued to the design-specified 125 ft-lbs, and the other with no nut on the bolt shank in order to model worst-case assembly con-

TABLE 1 FLEXURAL TEST RESULTS FOR COMPOSITE PLATE/RIB SECTIONS

(a) 0.125-in. Al. Plate with Type I Ribs @ 8-in. O.C.:

Test No.	Theoretical M_p (k-ft/ft)	Test Result M_{ult} (k-ft/ft)	M_{ult}/M_p (%)	Failure Mode
A-7	8.52	9.81	115	Rib Rotation
A-8	8.52	9.81	115	Rib Rotation
A-9	8.52	9.81	115	Rib Rotation

Avg. = 115%

(b) 0.125-in. Al. Plate with Type I Ribs @ 16-in. O.C.:

Test No.	Theoretical M_p (k-ft/ft)	Test Result M_{ult} (k-ft/ft)	M_{ult}/M_p (%)	Failure Mode
A-1	4.54	4.73	104	Rib Rotation
A-2	4.54	4.58	101	Rib Rotation
A-3	4.54	4.83	106	Rib Rotation

Avg. = 104%

(c) 0.125-in. Al. Plate with Type V Ribs @ 8-in. O.C.:

Test No.	Theoretical M_p (k-ft/ft)	Test Result M_{ult} (k-ft/ft)	M_{ult}/M_p (%)	Failure Mode
B-1	14.60	17.64	120	Rib Flange Crack
B-2	14.60	17.18	118	Rib Flange Crack
B-3	14.60	17.10	117	Rib Flange Crack

Avg. = 118%

(d) 0.125-in. Al. Plate with Type I/Type V Rib Splices @ 8-in. O.C.:

Test No.	M_{ult} (k-ft/ft) at First Bolt*	M_{max} (k-ft/ft) at Mid-Splice	M_{ult}/M_1 (%)	M_{ult}/M_5 (%)
C-1	11.41	12.01	134	78
C-2	11.27	11.86	132	77

Avg. = 133% Avg. = 77%

$M_1 = M_p$ (design) for Type I ribs @ 8 in. O.C. on 0.125-in. plate.

$M_5 = M_p$ (design) for Type V ribs @ 8 in. O.C. on 0.125-in. plate.

*Moment at Splice Bolt nearest the Type I-Only Rib Section.

TABLE 2 DESIGN MOMENT CAPACITIES FOR COMPOSITE PLATE/RIB SECTIONS: 0.125-IN. ALUMINUM PLATE WITH TYPE I OR TYPE V RIBS

Rib Spacing (in., O.C.)	Type I Ribs M_p-Design (k-ft/ft)	Type V Ribs M_p-Design (k-ft/ft)	Type I/Type V Splice Section M_p-Design (k-ft/ft)
6	11.08	18.91	11.08
8	8.52	14.60	8.52
12	5.91	10.11	5.91
16	4.54	7.97	4.54

TABLE 3 RESULTS OF BOLT PULL-THROUGH TESTS FOR 0.125-IN. ALUMINUM PLATE TESTED WITH STREAMLINED BOLT HEADS

Test No.	Test Conditions	Bolt Pull-Through Capacity (lbs)
1-T	Bolt + torqued nut	5,035
2-T	Bolt + torqued nut	5,025
3-T	Bolt + torqued nut	5,225
4-T	Bolt + torqued nut	5,175
Avg.		5,115
1	Bolt without nut	4,160
2	Bolt without nut	4,260
3	Bolt without nut	4,580
4	Bolt without nut	4,280
Avg.		4,320

ditions. The bolt heads that were pulled out through the sheets were the streamlined bolt heads shown in Figure 2b. The results of these tests are presented in Table 3. Based on these tests, a design value of 4,300 lbs/bolt for bolt pull-through capacity was adopted.

A third set of laboratory tests was performed to evaluate the deformations induced by normal pressures applied to the exterior of the smooth lining plates. This pressure results in inward deflections of the plate between bolt locations and will hereafter be referred to as plate "dimpling." To evaluate plate dimpling, composite plate/rib crown sections were assembled in lengths of 48-in. (along the culvert flow direction) and widths of 60 in. (across the culvert span) with the maximum design rib spacing of 16-in. o.c. Air bags were then used to apply a uniform pressure to the exterior faces of these composite plate/rib sections.

The maximum air bag pressure that could be applied (22 psi) represented a bolt loading of only approximately 75 percent of the (conservative) design bolt pull-through capacity, so these air bag tests could not be taken to the point of bolt pull-through failure. The purpose of these tests, however, was to evaluate plate dimpling between bolt support points, and it was judged that such dimpling was sufficiently minimized (plate face inward deflection less than 0.25 in.) at a limiting applied pressure of less than approximately one-half of the value representing full mobilization of the design bolt pull-through capacity. It was thus concluded that the use of a minimum factor of safety of 2.0 for bolt pull-through would also result in acceptable plate dimpling behavior.

SMOOTH-WALLED BOX DESIGN BASED ON THE SIMPLIFIED DESIGN METHOD

The development of final designs and a final fill height table for the proposed new family of smooth-walled box structures was based on providing adequate structural capacity with regard to the following:

1. Flexural capacity at the crown and haunch sections,
2. Haunch section axial thrust capacity, and
3. Bolt pull-through failure.

On the basis of shape similitude between the proposed new smooth-walled box structures and existing corrugated metal box culverts, it was assumed that the design moment calculations of the Simplified Design Method (SDM) proposed by Duncan et al. (*2*) would also apply to the new smooth-walled box structures. The SDM design procedures are based on incremental nonlinear finite element analyses of corrugated metal box culverts augmented by full-scale prototype backfill and live load tests. The SDM design equations result in calculations of (a) maximum backfill-induced crown and haunch moments (M_{CB} and M_{HB}) and (b) maximum live-load-induced moment increases in the haunch and crown regions (ΔM_{CL} and ΔM_{HL}) based on an HS-20 design live load. Load factors of 1.5 and 2.0 are then applied to the backfill- and live-load-induced moments, respectively, to develop the required design moment capacities for the box culvert crown and upper haunch regions as

$$M_{CD} = (1.5)(M_{CB}) + (2.0)(\Delta M_{CL}) \quad (1)$$

$$M_{HD} = (1.5)(M_{HB}) + (2.0)(\Delta M_{HL}) \quad (2)$$

The heavy solid lines in Figures 5 and 6 represent the SDM-required design moment capacities of the box culvert crown and upper haunch regions, respectively, as a function of culvert span and crown cover depth. Also shown on these figures (with dashed horizontal lines) are the actual design moment capacities (M_P) of the crown and upper haunch regions for composite plate/rib sections with rib spacings of 6-, 8-, 12-, and 16-in., as summarized previously in Table 2. Design of a smooth-walled box structure of a given span and range of crown cover depths is then accomplished by selecting a rib spacing such that the actual design moment capacities of both the crown and haunch regions exceed the required design moment capacities.

The second design consideration for smooth-walled box structures is the provision of adequate structural capacity to sustain axial thrust loading in the lower haunch region. In estimating haunch thrust loads, an adverse arching factor of 1.3 was conservatively assumed for backfill loads, and the HS-20 design live load (32 kips on a single axle) was treated as a 32-kip line load with a 6-ft width, which might occur almost directly over one of the haunches so that essentially the full live load would be carried by the haunch in thrust. Haunch thrust (P_H) was thus calculated as

$$P_H = (1.3)(H_C)(S)(\gamma_{bf})(0.5) + \frac{(LL)}{6\text{ ft}} \quad (3)$$

where

P_H = axial haunch thrust (kips/ft),
H_C = crown cover depth (ft),
S = box culvert span (ft),
γ_{bf} = unit weight of backfill (kips/ft^3), and
LL = live load (kips).

The basis of the axial haunch thrusts calculated using Equation 3, it was found that for combinations of smooth-walled box spans, cover depths, and rib spacings satisfying Equations 1 and 2 (moment design criteria), the maximum haunch thrusts developed were less than one-third of the axial thrust capacity

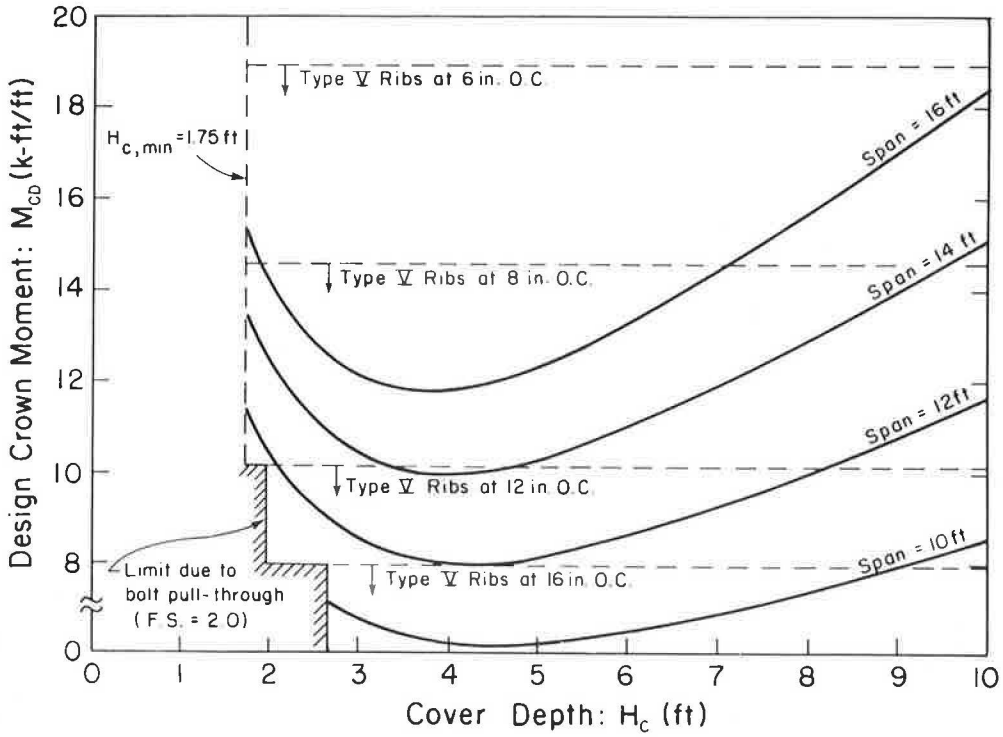

FIGURE 5 Comparison of design crown moment versus crown moment capacity for a range of spans, cover depths, and Type V rib spacings.

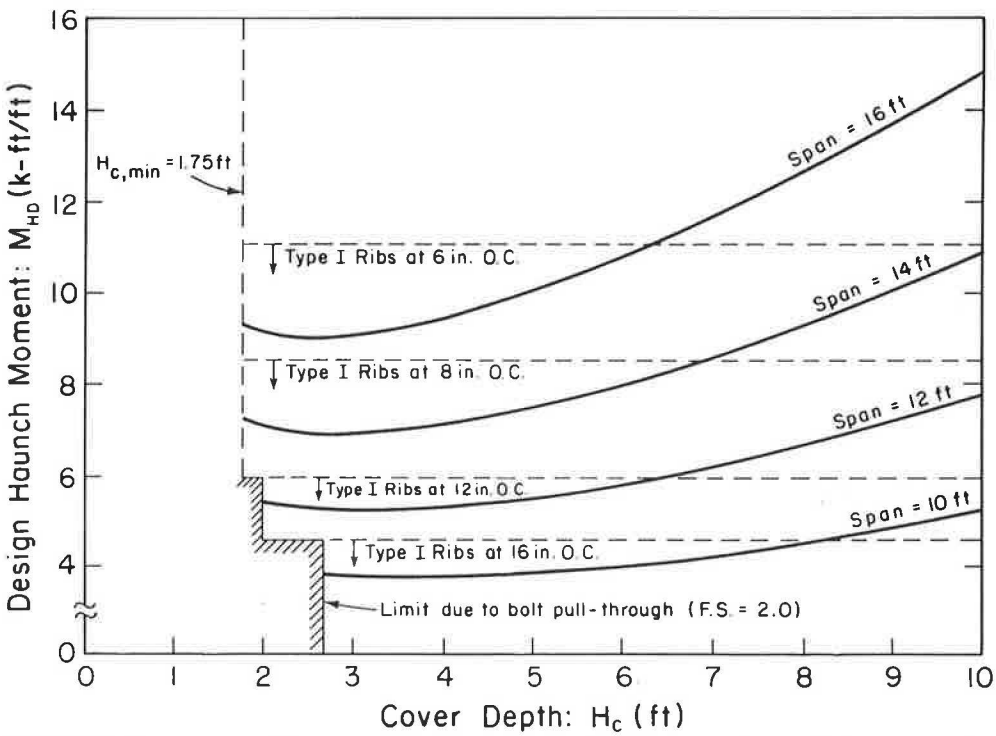

FIGURE 6 Comparison of design haunch moment versus haunch moment capacity for a range of spans, cover depths, and Type I rib spacings.

provided by the (Type I) haunch ribs. Therefore, by simply satisfying the flexural design criteria of Equations 1 and 2, a factor of safety of FS > 3 was also provided for potential haunch thrust failure.

The third design criteria for smooth-walled box structures is the provision of an adequate factor of safety with respect to bolt pull-through failure. A minimum factor of safety of FS ≥ 2 with respect to bolt pull-through was selected for design. As discussed in the previous section, this criterion and factor of safety also serve to adequately minimize plate dimpling between bolt points. For all spans and cover depths considered, the most critical conditions (largest normal pressures against the exterior of the smooth plate) occurred in the central crown region, directly beneath an HS-20 design load at minimum crown cover. The bolt pull-through design criteria thus served to establish the minimum allowable crown covers as a function of crown rib spacing.

Boussinesq-type vertical stress distribution analyses of three-dimensional live loads were used to evaluate crown bolt pull-through loads for various rib spacings and crown cover depths. Live loading was modeled as a conservatively modified HS-20 design load, in that four wheel loads of 8 kips each on a single axle were assumed to occur over an axle length of only 4.5 ft (at uniform 18-in. spacing), and a 50 percent impact factor was employed. Appropriate allowance was made for the partial shielding of the 2.6-in.-wide flanges of the Type V crown ribs. Design was based on an ultimate bolt pull-through capacity of 4,300 lb/bolt. Design was controlled by the minimum crown cover necessary to spread the concentrated live wheel loads. These bolt pull-through design criteria established the minimum allowable crown cover depths shown on Figures 5 and 6.

FINITE ELEMENT ANALYSIS STUDIES FOR DESIGN VERIFICATION

The design approach described in the preceding section was based largely on the SDM design methodology proposed by Duncan et al. (*2*). The SDM methodology was, in turn, based on nonlinear finite element analyses of conventional corrugated box culverts, augmented by full-scale prototype backfill and live load tests. The new smooth-walled box structures and existing corrugated metal box structures have similar geometries at the haunches and haunch/crown transition regions: haunch legs are straight and incline inward at varying angles, and the upper haunch/crown transition corner is a large-radius continuous curve. There is, however, a potentially significant difference between the crown region geometries of the smooth-walled and conventional corrugated box culverts: the corrugated culvert crowns are a single, large radius curve, while the smooth-walled box culvert crowns are a series of straight sections with bends between straight segments. A single bend occurs at midspan for smooth-walled boxes with spans of less than approximately 12 ft, and two bends occur at approximately the one-third-span points for smooth-walled boxes with longer spans.

Incremental nonlinear finite element analyses were performed to evaluate the effects of these differences in geometry on the safety and applicability of the SDM design methodology to the new smooth-walled box structures. Finite element analyses of a number of smooth-walled box culverts were performed using the program SSCOMP (*3*), a plane strain finite element code for incremental nonlinear analysis of soil-structure interaction. One-half of a typical finite element mesh used for these analyses is shown in Figure 7. Soil elements

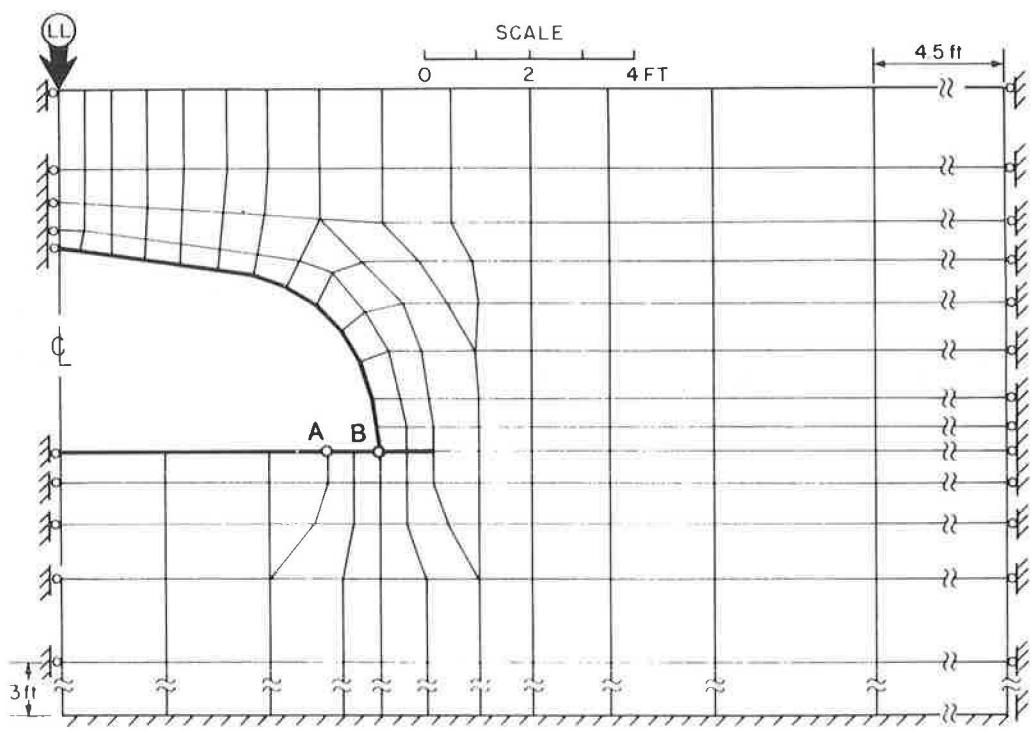

FIGURE 7 Typical finite element mesh for analysis of a smooth-walled box structure (structure Type "L").

were modeled with four node isoparametric elements, and the culvert structures were modeled with piece-wise linear beam elements. Nonlinear stress-strain and volumetric strain soil behavior was modeled using the hyperbolic formulation proposed by Duncan et al. (*4*) as modified by Seed and Duncan (*5*). Structural behavior was modeled as linear elastic. The analyses were performed in steps to incrementally model the actual backfill placement process and then the application of design live loading.

Structural parameters used to model the various culvert section components are listed in Table 4. Section moduli used to model the corrugated aluminum plate sections are based on large-scale flexural test data. Section moduli for these ribbed sections were modeled as equal to 80 percent of the theoretical flexural stiffness for the ribs and plate acting as a composite beam. Discrete vehicle loads were represented by equivalent line loads using the equivalent line load estimation procedure proposed by Duncan et al. (*2*) as modified by Seed and Raines (*1*). The design load used in all analyses was based on the standard 32-kip HS-20 single axle design load.

TABLE 4 SMOOTH-WALLED BOX CULVERT STRUCTURAL PROPERTIES MODELED

Rib Spacing (in., o.c.)	Modulus E (kip/ft^2)	Area A (ft^2/ft)	Moment of Inertia I ($\times 10^{-4}$)(ft^4/ft)
(a) Crown Region (Type V Ribs on 0.125-in. Al. Plate)			
6	1,468,800	0.042	3.85
8	1,468,800	0.034	2.72
12	1,468,800	0.026	2.28
16	1,468,800	0.022	1.84
(b) Haunch Region (Type I Ribs on 0.125-in Al. Plate)			
6	1,468,800	0.033	2.11
8	1,468,800	0.028	1.58
12	1,468,800	0.022	1.23
16	1,468,800	0.019	0.97
(c) Haunch/Crown Transition Region (Type I/Type V Rib Splice on 0.125-in. Al. Plate)			
6	1,468,800	0.050	4.62
8	1,468,800	0.041	3.26
12	1,468,800	0.031	2.74
16	1,468,800	0.026	2.21

The first series of analyses performed were for a Type "L" smooth-walled box, a structure with a span of 12 ft, 4 in. and a rise of 3 ft, 6 in. This structure has an average span and rise among the ranges of spans and rises proposed for the new smooth-walled box structures. This average structure was analyzed to establish worst case modeling criteria for a range of conditions. Modeling included the following:

1. A range of final crown cover depths,
2. A range of backfill properties,
3. A range of conditions of rotational fixity at the juncture of the haunch footing and invert section (Point A in Figure 7),
4. A range of conditions of rotational fixity at the base of the haunch stem (Point B in Figure 7), and
5. Conditions of either perfect soil/structure adhesion or a nonlinear, frictionally dependent soil/structure interface.

Two sets of backfill and foundation soil properties were modeled, representing (a) a silty clay of low plasticity compacted to 90 percent of the Standard Proctor (ASTM D-698) maximum dry density and (b) a well-compacted, well-graded gravelly backfill. The parameters used to model these two soils (CL-90 and GW-100) are listed in Table 5. The CL-90 parameters represent the lowest quality backfill currently allowed, and the GW-100 parameters represent a high-quality granular backfill, but also one with unusually high unit weight.

Fixity conditions at the juncture of the haunch footing and invert section were modeled as both (a) fully flexible hinge and (b) fixed (full moment transfer) connection. This range of variations was found to have little impact on calculated bending moments and axial thrusts in the box structure's crown and haunch regions. Fixity conditions at the base of the haunch leg were also modeled as either hinged or fixed, and this modeling was found to have some small effect on calculated crown and haunch moments and thrusts.

The calculated backfill-induced bending moments and HS-20 live-load-induced moment increases in both the crown and haunch sections of a Type "L" smooth-walled box for crown cover depths of 1.5 ft and 5.0 ft are listed in Table 6. Similar analyses performed for cover depths of 3.0 and 8.0 ft, are not included herein due to space limitations. The resulting moments are then scaled by load factors of 1.5 (for backfill loads) and 2.0 (for live loads) to produce the resulting factored crown and haunch design moments as in Equations 1 and 2. These

TABLE 5 HYPERBOLIC SOIL MODEL PARAMETERS USED IN FINITE ELEMENT ANALYSES

	γ (lb/ft^3)	K	n	R_f	K_b	m	c (lb/ft^2)	ϕ (deg.)	$\Delta\phi$ (deg.)
Maximum quality backfill: low-plasticity silty clay compacted to 90% R.C. (Standard AASHTO) (CL-90)	125	90	0.45	0.7	80	0.2	200	30	0
Maximum quality backfill: well-graded gravel compacted to 100% R.C. (Standard AASHTO) (CW-100)	145	450	0.4	0.7	125	0.2	0	39	7
Field test backfill: silty sand compacted to 95% R.C. (Standard AASHTO) (SM-95)	125	450	0.25	0.7	350	0.0	100	34	6

TABLE 6 COMPARISON OF SDM-BASED DESIGN MOMENTS AND MOMENTS CALCULATED BY NONLINEAR FINITE ELEMENT ANALYSES (SMOOTH-WALLED BOX STRUCTURE TYPE "L")

(a) DEPTH OF CROWN COVER = 1.5 ft:

CASE	CROWN			HAUNCH		
	BACKFILL MOMENT M_{CB} (k-ft/ft)	LIVE LOAD MOMENT ΔM_{CL} (k-ft/ft)	DESIGN MOMENT M_{CD} (k-ft/ft)	BACKFILL MOMENT M_{HB} (k-ft/ft)	LIVE LOAD MOMENT ΔM_{HL} (k-ft/ft)	DESIGN MOMENT M_{HD} (k-ft/ft)
DUNCAN, SEED & DRAWSKY (1984) PROPOSED MOMENTS: CL-90 MATERIAL	0.8	5.0	11.1	0.6	2.4	5.7
FINITE ELEMENT ANALYSIS: CL-90 MATERIAL, HINGED BASE, NO INTERFACE ELEMENTS	0.6	5.5	11.8	0.5	2.0	4.8
FINITE ELEMENT ANALYSIS: CL-90 MATERIAL, HINGED BASE, INTERFACE ELEMENTS	0.6	5.6	11.9	0.5	2.0	4.8
FINITE ELEMENT ANALYSIS: CL-90 MATERIAL, FIXED BASE NO INTERFACE ELEMENTS	0.7	5.2	11.5	0.6	1.8	4.5
FINITE ELEMENT ANALYSIS: GW-100 MATERIAL, FIXED BASE NO INTERFACE ELEMENTS	0.6	4.4	9.7	0.5	1.5	3.9
FINITE ELEMENT ANALYSIS: GW-100 BACKFILL OVER CL-90 FOUNDATION, HINGED BASE, NO INTERFACE ELEMENTS	0.7	4.6	10.3	0.6	1.5	3.9
FINITE ELEMENT ANALYSIS: CL-90 BACKFILL OVER FIRM FOUNDATION, HINGED BASE, NO INTERFACE ELEMENTS	0.5	4.6	9.9	0.5	1.8	4.4
FINITE ELEMENT ANALYSIS: CL-90 MATERIAL, HINGED BASE, NO INTERFACE ELEMENTS HS-20 LIVE LOAD OFF CENTER	0.6	4.5	9.8	0.5	1.8	4.4

(c) DEPTH OF CROWN COVER = 5.0 ft:

DUNCAN, SEED & DRAWSKY (1984) PROPOSED MOMENTS: CL-90 MATERIAL	2.8	1.8	7.7	2.0	1.3	5.6
FINITE ELEMENT ANALYSIS: CL-90 MATERIAL, HINGED BASE, NO INTERFACE ELEMENTS	1.7	1.0	4.5	1.6	0.8	4.0
FINITE ELEMENT ANALYSIS: CL-90 MATERIAL, HINGED BASE, INTERFACE ELEMENTS	1.7	1.0	4.6	1.6	0.8	4.0
FINITE ELEMENT ANALYSIS: CL-90 MATERIAL, FIXED BASE, NO INTERFACE ELEMENTS	1.8	0.9	4.6	1.7	0.8	4.1
FINITE ELEMENT ANALYSIS: GW-100 MATERIAL, FIXED BASE, NO INTERFACE ELEMENTS	1.4	0.5	3.2	1.3	0.4	2.8
FINITE ELEMENT ANALYSIS: GW-100 BACKFILL OVER CL-90 FOUNDATION, HINGED BASE, NO INTERFACE ELEMENTS	1.5	0.5	3.3	1.4	0.4	2.9
FINITE ELEMENT ANALYSIS: CL-90 BACKFILL OVER FIRM FOUNDATION HINGED BASE, NO INTERFACE ELEMENTS	1.4	0.8	3.8	1.4	0.7	3.5

factored design moments are also listed in Table 6, along with the factored design moments based on the SDM design methodology.

As shown in Table 6, the largest crown and haunch moments are calculated using the minimum quality CL-90 backfill. A flexible hinge at the base of the haunch leg tends to result in slightly higher crown and haunch moments than does a fixed haunch leg base. The modeling of a frictional soil/structure interface condition results in a negligible difference in crown and haunch moments as opposed to those calculated based on modeling perfect soil/structure interface adhesion. Although not listed in Table 6, haunch thrusts were appreciably larger when perfect soil/structure adhesion was modeled. In general then, the worst-case (or most conservative) modeling conditions were found to be those corresponding to modeling of a minimum quality (CL-90) backfill with a hinged haunch base connection and perfect soil/structure interface adhesion.

Similar analyses were performed for two additional smooth-walled box structures (with different geometries) for these worst-case conditions. These structures were (a) a Type "O" structure with a span of 13 ft, 3 in., and a rise of 5 ft, 11 in., and (b) a Type "W" structure with a span of 15 ft, 8 in. and a rise of 4 ft, 7 in. These structures represented (a) a smooth-walled box with an unusually high aspect ratio (rise vs. span ratio) and (b) a low aspect ratio structure with a relatively large span approaching the maximum spans proposed.

The resulting FEM-calculated crown and haunch moments for these two structures over a range of final crown cover depths are shown in Tables 7 and 8. Also shown for comparison purposes are the corresponding moments calculated on the basis of the SDM design methodology. As shown in Tables 6, 7, and 8, the FEM-calculated factored design moments in the crown region slightly exceed the SDM-based factored design moments (by 10 percent or less) for worst-case modeling conditions and minimum crown cover depths. At larger than minimum crown cover depths, the SDM-based factored design crown moments are larger than the FEM-calculated factored design moments, and the SDM-based haunch moments are larger than the FEM-based haunch moments at all crown cover depths.

At minimum cover depths, the factored design crown moments are dominated by the live-load-induced moment increases. As the worst-case FEM-calculated crown moments for the minimum cover conditions exceed the SDM-based moments by less than 10 percent, and both include a Load Factor of 2.0 for live-load-induced moment increases, it may be concluded that the SDM-based design provides a factor of safety of almost 2.0 with respect to crown failure in flexure under HS-20 loading for these worst-case minimum crown cover conditions. For all crown cover depths greater than these minimum allowable crown covers, the SDM-based crown and haunch design moments are conservative relative to the worst-case FEM-calculated moments. Accordingly, it was concluded that the SDM design methodology represented a suitable and adequately conservative basis for flexural capacity design of the proposed new smooth-walled box structures.

In addition to providing good support for the SDM-based flexural design of the new smooth-walled box structures, the finite element analyses also showed the axial thrusts at the bases of the culvert haunches, as estimated using Equation 3, to be conservative (larger) relative to those calculated by the finite element analyses for all culvert geometries, cover

TABLE 7 COMPARISON OF SDM-BASED DESIGN MOMENTS AND MOMENTS CALCULATED BY NONLINEAR FINITE ELEMENT ANALYSES (SMOOTH-WALLED BOX STRUCTURE TYPE "O")

	CASE	CROWN			HAUNCH		
		BACKFILL MOMENT M_{CB} (k-ft/ft)	LIVE LOAD MOMENT ΔM_{CL} (k-ft/ft)	DESIGN MOMENT M_{CD} (k-ft/ft)	BACKFILL MOMENT M_{HB} (k-ft/ft)	LIVE LOAD MOMENT ΔM_{HL} (k-ft/ft)	DESIGN MOMENT M_{HD} (k-ft/ft)
H_c=1.5 ft	DUNCAN, SEED & DRAWSKY (1984) PROPOSED MOMENTS	0.9	5.4	12.1	0.7	2.7	6.5
	FINITE ELEMENT ANALYSIS: CL-90 MATERIAL, HINGED BASE	0.3	5.9	12.2	0.5	1.9	4.6
H_c=3.0 ft	DUNCAN, SEED & DRAWSKY (1984) PROPOSED MOMENTS	1.9	3.0	8.9	1.4	2.0	6.1
	FINITE ELEMENT ANALYSIS: CL-90 MATERIAL, HINGED BASE	0.8	2.5	6.2	0.9	1.0	3.4
H_c=5.0 ft	DUNCAN, SEED & DRAWSKY (1984) PROPOSED MOMENTS	3.3	1.9	8.7	2.5	1.4	6.6
	FINITE ELEMENT ANALYSIS: CL-90 MATERIAL, HINGED BASE	1.5	1.1	4.4	1.4	0.6	3.4
H_c=8.0 ft	DUNCAN, SEED & DRAWSKY (1984) PROPOSED MOMENTS	5.3	1.4	10.8	4.0	1.1	8.1
	FINITE ELEMENT ANALYSIS: CL-90 MATERIAL, HINGED BASE	2.4	0.5	4.6	2.1	0.4	3.9

TABLE 8 COMPARISON OF SDM-BASED DESIGN MOMENTS AND MOMENTS CALCULATED BY NONLINEAR FINITE ELEMENT ANALYSES (SMOOTH-WALLED BOX STRUCTURE TYPE "W")

	CASE	CROWN			HAUNCH		
		BACKFILL MOMENT M_{CB} (k-ft/ft)	LIVE LOAD MOMENT ΔM_{CL} (k-ft/ft)	DESIGN MOMENT M_{CD} (k-ft/ft)	BACKFILL MOMENT M_{HB} (k-ft/ft)	LIVE LOAD MOMENT ΔM_{HL} (k-ft/ft)	DESIGN MOMENT M_{HD} (k-ft/ft)
H_c=1.7 ft	DUNCAN, SEED & DRAWSKY (1984) PROPOSED MOMENTS	1.4	5.9	14.0	1.2	3.4	8.6
	FINITE ELEMENT ANALYSIS: CL-90 MATERIAL, HINGED BASE	1.1	7.0	15.5	1.1	2.6	6.9
H_c=3.0 ft	DUNCAN, SEED & DRAWSKY (1984) PROPOSED MOMENTS	2.6	3.5	11.0	2.1	2.5	8.2
	FINITE ELEMENT ANALYSIS: CL-90 MATERIAL, HINGED BASE	1.9	3.4	9.6	1.9	1.7	6.3
H_c=5.0 ft	DUNCAN, SEED & DRAWSKY (1984) PROPOSED MOMENTS	4.4	2.2	11.0	3.6	1.8	9.0
	FINITE ELEMENT ANALYSIS: CL-90 MATERIAL, HINGED BASE	2.9	1.6	7.5	2.9	1.1	6.5
H_c=8.0 ft	DUNCAN, SEED & DRAWSKY (1984) PROPOSED MOMENTS	7.1	1.7	14.0	5.8	1.4	11.4
	FINITE ELEMENT ANALYSIS: CL-90 MATERIAL, HINGED BASE	4.2	0.7	7.7	4.3	0.6	7.7

depths, and combinations of modeling conditions considered. This finding supported the earlier conclusion that the provision of adequate flexural capacity in both the crown and haunch regions also resulted in the provision of adequate haunch thrust capacity (FS > 3) for these new smooth-walled box structures.

FULL-SCALE PROTOTYPE TEST AND ANALYSES

As an additional check on the design analyses described thus far, a full-scale prototype smooth-walled box structure was installed and subjected to an HS-20 field load test. The field load test structure, a Type "D" smooth-walled box structure with a span of 10 ft, 6 in., and a rise of 4 ft, 6 in., was installed as a roadway bridge across a creek near Charlotte, North Carolina. This structure, with ribs at 12-in. o.c., was backfilled to a final crown cover depth of 2.0 ft with a locally available silty sand backfill compacted to an average of approximately 94 percent of the Standard Proctor (ASTM D-698) maximum dry density.

After completion of backfilling, but before paving the overlying road surface, an HS-20 live load test was performed using a loaded dump truck with a rear axle load of 32 kips distributed on four wheels (two pairs of tandem wheels). The 32-kip rear axle was positioned directly over the smooth-walled box structure centerline, and the resulting maximum crown deflections were recorded. The central crown ribs deflected approximately 0.21 in. under the HS-20 load, and the flat plate between the ribs deflected approximately an additional 0.20 in. The live load was then removed from the structure, and the crown ribs rebounded elastically to rcover about one-half of their initial deflection, resulting in a residual deflection (set) of about 0.11 in. The 32-kip axle load was then driven 10 times across the structure, after which it was observed that crown deflections had ceased to increase with the number of passes. On the 11th pass, the dump truck was halted with its 32-kip rear axle again directly over the smooth-walled box centerline, and a maximum (net) crown rib deflection of about 0.28 in. was observed, of which a residual set of about 0.16 in. remained after load removal.

Incremental nonlinear finite element analyses, using the techniques described previously, were performed to model the incremental backfill placement and the subsequent initial HS-20 load application above the centerline of the backfilled structure. The soil parameters used to model the compacted silty sand backfill are listed in the third column of Table 5. These finite element analyses predicted an initial live-load-induced crown displacement of approximately 0.24 in., which was in excellent agreement with the 0.21 in. actually observed. Backfill- and live-load-induced haunch and crown moments calculated by these FEM analyses were smaller than those estimated based on the SDM design methodology. The results of this full-scale prototype live load test were thus judged to support the accuracy and conservatism of the finite element studies and SDM design procedures employed in the analysis and development of the new smooth-walled box structures.

Finally, the observed plate dimpling under repeated HS-20 live loading never exceeded a measured 0.3 in. incremental displacement of the flat plate face relative to the adjacent ribs. This relative displacement, which was barely discernible, was judged to represent acceptable performance with respect to plate dimpling.

SUMMARY AND CONCLUSIONS

The smooth-walled box structure system described in this paper represents a new approach to the problem of providing efficient transport of water beneath ground cover with limited crown clearances. The smooth walls of these strucutres provide significantly increased hydraulic efficiency over that achieved by current conventional corrugated metal box culverts. This hydraulic efficiency offsets the decreased structural efficiency (decreased flexural capacity) of the composite smooth plate/rib sections and permits the use of a significantly smaller smooth-walled box structure cross-sectional area to transport the same maximum design flow volume as would be transported by a significantly larger corrugated box culvert cross-sectional area. This smaller structure, in turn, minimizes overall structure size and cost, requires smaller clearances for installation under shallow cover constraints, and minimizes the excavation and backfill volumes required for installation.

The finite element analyses performed as part of these studies support the applicability of the SDM design methodology to the analysis and design of these new smooth-walled structures. The large-scale laboratory tests described provide a basis for evaluation of the various structural system component capacities necessary for design of these structures. Finally, a full-scale field prototype HS-20 live load test was performed and analyzed using the same finite element analysis modeling techniques used in the development and design of these new structures. The results of this full-scale prototype live load test provide good support for the accuracy of these finite element analysis techniques and for the suitability and conservatism of the design procedures proposed for these new smooth-walled box structures.

REFERENCES

1. R. B. Seed and J. R Raines. Failure of Flexible Long-Span Culverts Under Exceptional Live Loads. Presented at the 67th Annual Meeting of the Transportation Research Board, Washington, D.C. Jan., 1988.
2. J. M. Duncan, R. B Seed, and R. H. Drawsky. *Design of Corrugated Metal Box Culverts*. Geotechnical Engineering Research Report UCB/GT/84-10. University of California at Berkeley, July, 1984.
3. R. B. Seed and J. M. Duncan. *SSCOMP: A Finite Element Analysis Program for Evaluation of Soil-Structure Interaction and Compaction Effects*. Geotechnical Engineering Research Report UCB/GT/84-02. University of California at Berkeley, Feb., 1984.
4. J. M. Duncan, P. Byrne, K. S. Wong, and P. Mabry. *Strength, Stress-Strain and Bulk Modulus Parameters for Finite Element Analyses of Stresses and Movements in Soil Masses*. Geotechnical Engineering Research Report UCB/GT/80-01. University of California at Berkeley, Jan., 1980.
5. R. B. Seed and J. M. Duncan. *Soil-Structure Interaction Effects of Compaction-Induced Stresses and Deflections*. Geotechnical Engineering Research Report UCB/GT/83-06, University of California at Berkeley, Dec., 1983.

Publication of this paper sponsored by Committee on Subsurface Soil-Structure Interaction.